Fano interference for large-amplitude coherent phonons in bismuth

2007 J. Phys.: Condens. Matter 19 156227

(http://iopscience.iop.org/0953-8984/19/15/156227)

IOP PUBLISHING JOURNAL OF PHYSICS: CONDENSED MATTER

J. Phys.: Condens. Matter **19** (2007) 156227 (9pp) doi:10.1088/0953-8984/19/15/156227

Fano interference for large-amplitude coherent phonons in bismuth

O V Misochko[1], K Ishioka[2], M Hase[3] and M Kitajima[2]

[1] Institute of Solid State Physics, Russian Academy of Sciences, 142432 Chernogolovka, Moscow region, Russia
[2] National Institute for Materials Science, 1-2-1 Sengen, Tsukuba, Ibaraki 305-0047, Japan
[3] Institute of Applied Physics, University of Tsukuba, 1-1-1 Tennodai, Tsukuba 305-8573, Japan

E-mail: misochko@issp.ac.ru

Received 15 January 2007, in final form 22 February 2007
Published 27 March 2007
Online at stacks.iop.org/JPhysCM/19/156227

Abstract

We report femtosecond time-resolved measurements of lattice dynamics in bismuth made over a wide range of temperatures and excitation levels. We demonstrate that time-integrated Fourier transforms for both the fully symmetric A_{1g} and doubly degenerate E_g coherent oscillations of large amplitude exhibit asymmetric line shapes described by the Fano formula. Measuring the real and imaginary part of the phonon self-energy, we attempt to identify the nature of the continuum responsible for the configuration mixing. Based on the measured pump and temperature dependences, we suggest that the continuum responsible for the interference includes both the electronic and lattice degrees of freedom.

(Some figures in this article are in colour only in the electronic version)

1. Introduction

The interactions of a discrete state embedded in a continuum gives rise to an interference effect whose signatures are recognized as the Fano profile [1]. General interest in observing and analysing the Fano profiles is inspired by their high sensitivity to the details of the interaction process. This quantum interference is ubiquitous in many endeavours in physics and has been studied in such time-integrated measurements as nuclear resonance, atomic ionization, molecular dissociation, and optical scattering. Moreover, the recent progress in laser technology has allowed observing the nonstationary dynamics of quasiparticles by exciting the Fano resonance with an ultrashort pulse [2]. Accordingly, it is desirable to further expose the essence of the mechanism underlying the Fano interference through a time-resolved study, thereby complementing the insights obtained from the frequency domain.

Advances in generating coherent lattice states have stimulated activity aimed at the study of lattice dynamics near the Lindemann stability limit [3–10] (i.e., melting might be expected when the root mean vibration amplitude reaches at least 10% of the nearest-neighbour

distance). Recently, there have been several time-domain observations of large-amplitude coherent phonons in bismuth [3–6, 8–10]. Following intense, ultrafast photo-excitation, which results in both the dense electron–hole plasma and large-amplitude lattice distortion, the transient lattice state demonstrates intricate dynamics. In describing such transient behaviour controlled by the complex spatio-temporal dynamics of the phonons and charge carriers, one has to separate the relative importance of the contributions from non-equilibrium carrier concentration and lattice anharmonicity. Up to now this task has not been achieved, and there exist two competing points of view [10]. Attempting to explain one of the peculiar features observed for large-amplitude coherent phonons in Bi, namely the time-dependent down-shift of frequency, some groups relied exclusively on *lattice* anharmonicity [4, 11], while another [8] advocated dynamical screening [12], defined as a weakening of the restoring force due to *electronic* excitation [13]. However, at the high excitation level, not only the frequency, but also the decay pattern of coherent oscillations is transformed (i.e., both the position and *shape* of the phonon spectrum are grossly changed). Consequently, any model for large-amplitude coherent phonons disregarding the modified decay of the transient lattice state may lead to misleading assertions.

In this report we attempt to contribute to an understanding of large-amplitude coherent lattice dynamics. We present the results of a time-resolved study for two different symmetry phonons in bismuth demonstrating asymmetric line shapes observed in a nonlinear, large-amplitude regime. Using Fano's formula we determine both the real and imaginary parts of the phonon self-energy over a wide range of temperatures and excitation levels. The results obtained support our assumption that the origin of the asymmetric profiles is a Fano-like interference.

2. Experimental results and discussion

A detailed description of the experiment is given elsewhere [6, 9]. Compared to the data presented in [6, 9] a highly improved frequency resolution limited by the Nykvist frequency $\nu_N = 1/\Delta t$ has been obtained by extending the scanned delays Δt up to 80 ps. Additionally, we have employed two alternative detection schemes [14] to study separately coherent phonons of different symmetry. For temperature measurements, a single crystal of bismuth was mounted into a closed-cycle cryostat. A Ti:sapphire mode-locked laser at 800 nm was amplified using a regenerative 100 kHz amplifier. The output laser pulse had a duration of 150 fs and was divided into pump and probe parts. Both the pump and probe beam were kept close to normal incidence and focused to a spot diameter of 0.1 mm by a single lens.

Before describing our experiment it is perhaps useful to present a simple picture of what occurs. The bismuth crystal structure is rhombohedral (A7), with two atoms per unit cell. The A_{1g} phonon corresponds to the out-of-phase displacement of these two atoms against each other along the trigonal axis, while the E_g phonon consists of out-of-phase movements in the plane perpendicular to the A_{1g} displacement. We excite the E_g and A_{1g} phonons in a time that is short compared to phonon lifetimes and their inverse frequencies. The first condition means that we are dealing with a transient lattice state, while the second is responsible for the coherent nature of the lattice excitation. There are two main processes responsible for the creation of coherent phonons. After ultrafast excitation, a significant fraction of the valence electrons are excited to higher electronic states. Such excitation greatly reduces the attractive part of the interatomic potential and allows the atoms to move with their thermal velocities towards a new equilibrium state even though the centre of mass, collectively, is still in the undisturbed position [15]. Simultaneously, since the spectral bandwidth of the ultrashort pulse exceeds the phonon frequency, such a pulse exerts a temporally impulsive driving force on the lattice atoms.

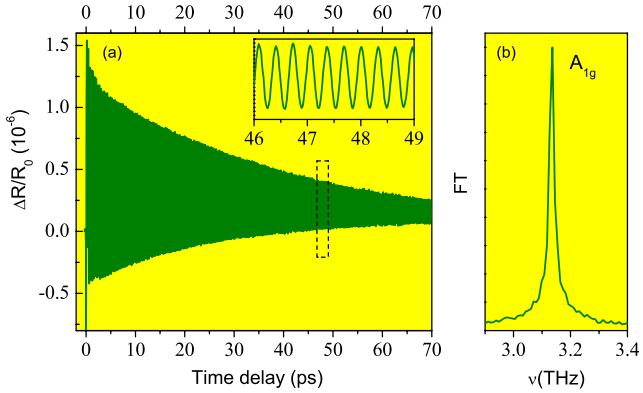

Figure 1. (a) Differential change in reflection at $T = 7$ K showing the coherent oscillation taken with seed light ($F = 0.01$ mJ cm^{-2}, repetition rate 82 MHz, $\Delta t = 70$ fs) in the isotropic detection. The polarization of the pump parallel to the trigonal axis excludes the excitation of doubly degenerate phonons. The dashed rectangle indicates the range of the scan shown in the inset. (b) Fourier transform of the oscillatory signals in panel (a).

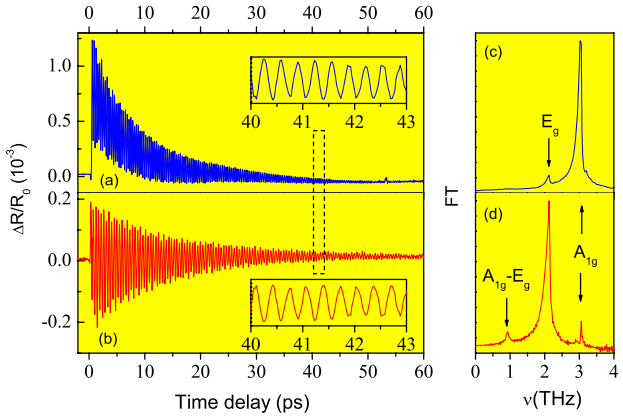

Figure 2. Differential change in reflection at $T = 10$ K showing the coherent oscillation of large amplitude for isotropic ((a), blue) and anisotropic detection ((b), red). Average power of an amplified Ti–sapphire laser $P = 0.5$ mW, repetition rate 100 kHz, and $\Delta t = 150$ fs, pump polarization parallel to the bisectrix axis. The dashed rectangle indicates the range of the scan shown in the insets. (c), (d) Fourier transforms of the oscillatory signals in (a) and (b), respectively.

This force gives a kick to the atoms, changing their thermal velocities. These two contributions leading to a change in either the potential or kinetic energy can be straightforwardly understood in the Raman scattering framework [16, 17].

In the isotropic pump–probe measurements, we detect the reflected probe beam of the same polarization as the incident beam, and the difference between the signal (with sample) and reference (without sample) is recorded. Here one measures the diagonal elements of the Raman tensor a_{ij} and the typical pump–probe data shown in figures 1(a) and 2(a) consist of two contributions. The first is non-oscillating (presumably electronic), while the second is an oscillating (lattice) response. At low excitation and liquid helium temperature, the oscillatory response of A_{1g} symmetry dominates and its time-integrated Fourier transform (FT) exhibits an almost symmetric line shape; see figure 1(b). Increasing excitation does not change either the frequency or decay time up to the excitation level of the order of 100 μJ cm^{-2}. Further

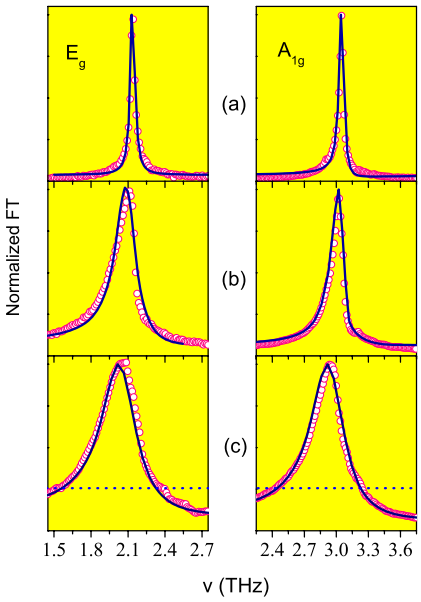

Figure 3. Line shapes of the A_{1g} and E_g phonons for different excitation levels: (a) $P = 1$ mW, (b) $P = 2.5$ mW, (c) $P = 7.5$ mW. The open symbols represent the experimental points, and the solid lines are the Fano line shapes computed with equation (1), whereas the dotted lines in the lower panels mark the base-line level.

increase in the pump power results in a faster, non-exponential decay and a slight down-shift of the oscillation frequency. This leads to an asymmetric line shape in the FT spectrum with more spectral weight at the low-frequency wing; see figures 2(c) and 3. At a higher excitation, the asymmetry and down-shift in frequency become more pronounced, and finally, near the Lindemann stability limit, the oscillations demonstrate either a collapse and revival [6], or a simple biexponential decay [9], depending on the duration and presumably the chirp of the laser pulse.

In the anisotropic measurements, the probe beam is polarized 45° with respect to the bisectrix axis, and after reflection it is analysed in two polarizations (parallel to the bisectrix and parallel to the binary axis), with the difference between the two components being recorded. In this detection scheme, where the difference $a_{xx} - a_{yy}$ between the Raman tensor components is measured, the dominant part of the signal comes from the lattice contribution of E_g symmetry; see figures 2(b) and (d). The almost complete suppression of the electronic (non-oscillating) part proves that the electronic response in the time domain has essentially full symmetry since it cancels out in the anisotropic detection. In the anisotropic detection, the time-integrated FT of the oscillations is dominated by the doubly degenerate E_g phonons with the difference A_{1g}–E_g mode present at moderate and high excitations. Their asymmetric line shapes as well as those for the A_{1g} phonons detected with the isotropic detection are suggestive of the Fano interference [1] between a discrete phonon level and a continuum.

In the Fano effect, two paths from the given state of a system—one direct from the discrete (in our case, phonon) state and one mediated by a continuum—interfere to produce an asymmetric line shape given by [18]

$$f(\varepsilon) = \frac{(\varepsilon + q)^2}{1 + \varepsilon^2} \tag{1}$$

where q is the asymmetry parameter and the dimensionless energy ε is used to measure the

energy difference from a renormalized phonon frequency ν_d in terms of its half-width $\Gamma/2$. The parameters q, ν_d and Γ are given by

$$q = \frac{V(T_d/T_c) + V^2 R(\varepsilon)}{\pi V^2 \rho(\varepsilon)}; \qquad \Gamma = V^2\rho(\varepsilon) + \gamma; \qquad \nu_d = \nu_0 - V^2 R(\varepsilon) \tag{2}$$

where T_d and T_c are the transition amplitudes for the decoupled phonon and continuum, respectively, $\rho(\varepsilon)$ the density of continuum states, $\pi^{-1}R(\varepsilon)$ its Hilbert transform, V the interaction strength, and γ the inverse lifetime of the unperturbed discrete level. In other words, the continuum due to the interaction V acquires a structure in the energy 'window' defined by γ. The self-energy due to phonon–continuum mixing is $\Sigma(\upsilon) = V^2[-R(\varepsilon) + i\rho(\varepsilon)]$, where the real part of Σ is the frequency shift of the unperturbed discrete level ν_0 and the imaginary part the broadening.

Let us first consider the spectra obtained in the both detection schemes for various excitation levels. The evolution of line shapes as a function of pump power is highlighted in figure 3 at three representative pump powers. The six graphs, together with figure 1(b), are designed to serve as an illustration of the transition from an almost symmetrical Lorentzian-like peak to a significantly wider asymmetric Fano-like profile at a higher excitation. It is interesting to note that the asymmetric line shape was observed in Te, where it was explained by the strong inhomogeneity of the initial photoexcited carrier density (i.e., the delayed pulse probes the contributions from different depths perpendicular to the surface where the carrier densities are varied) [19]. Such a conclusion was supported by the results of two pulse experiments, which demonstrated that the A_1 oscillation frequency in Te is completely defined by the excited carrier density. However, the widely used idea that lattice dynamics depend on the excited carrier density alone is an approximation that holds only when (i) the carriers can thermalize before any significant lattice motion occurs and (ii) the electronic state and the lattice state evolve independently after ultrafast excitation. The first is true for both Bi and Te: carriers thermalize within 10–100 fs, leading to a Fermi–Dirac distribution and a complete loss of memory of the initial excited carrier configuration. Nevertheless, the second condition, most likely realized for Te, breaks down for Bi. Indeed, the different lattice dynamics in the case of two-pulse excitation in Bi [10] reflect the fact that the potential energy surface on which Bi atoms move is determined not only by the number and/or distribution of the excited carriers, but also by the existing lattice deformation; see also [11]. Thus, we believe that the phonon line shape in Bi cannot be explained in a way similar to Te, i.e., the inhomogeneity of the initial carrier density alone cannot account for the phonon asymmetry.

We fitted the experimental data at all excitation levels to equation (1), where q, ν and Γ were treated as adjustable parameters. To extract the real and imaginary parts of the phonon self-energy we used Γ and ν_0 from the spontaneous Raman data and low-fluence experiments [14, 20], in which the continuum effects are thought to be negligible. The pump dependence of the asymmetry parameter q and the phonon self-energy Σ is shown in figures 3(c) and (d) for the two modes. The asymmetry parameter for A_{1g} coherent phonons initially grows as a square route of pump power and then saturates at a higher ($P > 7$ mW) excitation level. We find that Im Σ increases approximately quadratically with pump power; the fit shown in figure 3(c) yields Im $\Sigma = (0.08 + 0.0016P^2)$ THz, with P in mW. At the same time the frequency shift related to Re Σ increases at higher excitation. For E_g coherent phonons, the asymmetry parameter and self-energy evolve in a similar way. Like the A_{1g} phonons in figure 3(c), the E_g phonons have a smaller value of $|q|$ and a larger Σ at higher excitation. We find that the self-energy of the doubly degenerate phonons is less pump dependent than that of the fully symmetric phonons. For instance, the E_g broadening increases with power as Im $\Sigma = (0.03 + 0.001P^2)$ THz.

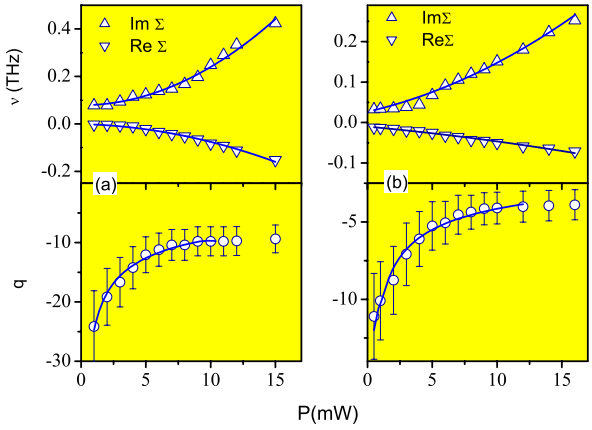

Figure 4. The real and imaginary parts of the self-energy and the asymmetry parameter q for the A_{1g} (a) and E_g (b) coherent phonons as a function of pump power. The solid lines are the fits described in the text.

We also studied the Fano parameters as a function of temperature for fully symmetric A_{1g} coherent phonons. The overall behaviour shown in figure 5 is as follows: at higher temperature the line shape becomes slightly more asymmetric, whereas the self-energy effects are not negligible. More exactly, in the temperature range from 7 to 300 K, the asymmetry parameter is either independent of or only slightly dependent on temperature (given the large error bars we cannot make a more definite conclusion). However, we observe that the self-energy varies with temperature even in a temperature range for which q is approximately constant. Over the measured temperature range, Im Σ increases substantially with increasing temperature (it grows slightly from 7 K to about 80 K and then increases approximately linearly with T above 80 K). We found that a good fit to Im Σ is obtained by

$$\text{Im}\,\Sigma(T) = \gamma_0\left(1 - \frac{2}{e^{\frac{h\nu}{2kT}} - 1}\right) \tag{3}$$

with $\nu = 3$ THz. The excellent fit in figure 5(a) is compatible with a temperature-dependent lifetime that is dominated by a Bose–Einstein statistical factor. The absence of any sharp changes in phonon frequency as a function of temperature is also consistent with this interpretation. |Re Σ| increases approximately linearly with temperature. The decrease in the phonon frequency with increasing temperature is probably caused by lattice anharmonicity (that is, lattice thermal expansion).

The good quality of the fits shown in figure 3 together with the trends in the values observed in figures 4 and 5 confirmed that the change in the phonon spectrum at high excitation level could be explained with the Fano profile. Such characteristics of the line shape at high excitation level as strong asymmetry, increase of line width, spectral response below the base-line level, and shift of frequency support our hypothesis. We discuss first the values of the asymmetry parameters, their sign, and their change with increasing excitation. The scaled behaviour for the Fano parameters of both modes is suggestive that the fully symmetric and doubly degenerate phonons interact with the continua of similar nature. The sign of q is in all cases negative, implying that the phonon and continuum polarizabilities have different signs (note that spontaneous Raman measurements on Sb [21] revealed that the sign of q for the E_g mode was positive). The decrease of $|q|$ with increasing pump power can indicate an increase of interaction V, while the subsequent saturation is suggestive of blocking the channel responsible for the preparation of the continuum.

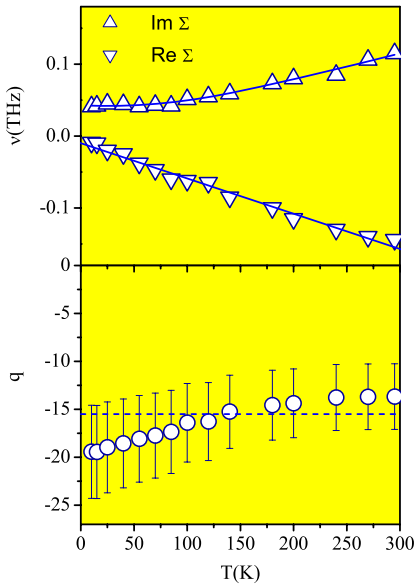

Figure 5. The real and imaginary parts of Σ and the asymmetry parameter q for the A_{1g} coherent phonons as a function of temperature. The solid lines in the upper panel are the fits described in the text. The dashed line in the bottom panel is just a guide to the eye.

Now let us try to identify the nature of the continuum. The electronic part of the continuum can be due to interband and intraband transitions. The Fermi surface in Bi and the band structure away from the Fermi level are known fairly well as a result of many theoretical investigations [22–24]. The Fermi level crosses the bands near the symmetry points T and L, creating there the hole and electron pockets. However, since we have observed similar asymmetric line shapes in Sb, where interband transitions do not overlap with phonon frequencies [22, 23], we tentatively ascribe the electronic contribution to intraband scattering. Furthermore, the observed saturation of q at high excitation can be related to a filling of the hole pocket, and thus the main electronic contribution to the continuum is thought to be due to the intraband scattering at the T point. It should be noted, however, that for E_g coherent phonons the interference with the intraband continuum would be hindered by symmetry reasons [18] and, moreover, as mentioned above, the sign of q for the E_g mode observed by spontaneous Raman scattering in Sb is positive [21]. However, apart from the charge carriers, one has to consider the lattice contribution to the continuum. The actual lattice state may be regarded as a superposition of states of different normal modes obtained in the independent particle approximation. These modes are mixed by the interaction defined by terms of the Hamiltonian disregarded in the harmonic approximation. This lattice anharmonicity manifests itself primarily in the phonon lifetime, which is an intermode effect involving a continuum of acoustic phonon states. The temperature dependence of the Fano parameters suggests that the acoustical modes coupled through the lattice anharmonicity to optical phonons contribute to the phonon self-energy, but not to the interference. Thus, the acoustic continuum is an additional continuum in the Fano problem [1] which is responsible only for diagonal phonon decay. This is always the case in inelastic scattering [18] and it occurs since the expressions for Σ and q are independent of each other. However, in addition to the intermode anharmonicity, the lattice atoms participating in large-amplitude oscillations spend an appreciable fraction of time in the region where the potential is strongly anharmonic. This makes the situation quite similar to that with molecules

where the anharmonicity results in a set of discrete levels with non-equidistant spacings. Such type of anharmonicity results in a quasicontinuum (a collection of closely spaced levels which originate from different number states of *each* phonon mode). The symmetry of such quasicontinuum coincides with that of the phonon mode; therefore, interference between the discrete level and the continuum is always possible. Furthermore, the quasicontinuum term with level spacing roughly inversely proportional to the coherent amplitude gives a memory to the continuum, which can maintain enough coherence to modify the discrete-continuum interaction through *repeated* phonon–continuum interactions.

Finally, we will try to explain the transition from small-amplitude coherent oscillations, which give the same decay rate as spontaneous Raman data [20], to large-amplitude ones, where the dynamics are more complex. At low excitation level, $V^2\rho(\varepsilon) \leqslant \gamma$; therefore, the 'window' size (i.e., the energy range in which the continuum is modified by the interaction) is defined by diagonal relaxation. As a result, the dynamics in the time domain are the same as in the frequency domain. For a high excitation level, $V^2\rho(\varepsilon) \geqslant \gamma$ leads to a wider 'energy window' in the Fano model, thereby resulting in a stronger interaction with the continuum. In this nonlinear regime, the relation between the diagonal and off-diagonal relaxation $\gamma_{\mathrm{d}}/\gamma_{\mathrm{od}} = 2$ breaks down, and the 'window' size starts to be controlled by off-diagonal relaxation [25]. It is immediately clear that the original Fano model should be modified in two aspects for the time domain. First, coherence should be included in the model in order to explain an extended energy range of the continuum modified by electron–phonon interaction at higher excitation. Second, the quasicontinuum term should be taken into account. A similar problem has been solved for the autoionization in a strong laser field [25–27] and, hopefully, it can be extended to the results obtained for large-amplitude coherent phonons in the time domain. Within such a scenario, the short-time dynamics can be governed by a continuum term, which mainly includes the contribution of charge degrees of freedom. For longer time, when the discreteness of the continuum has been revealed, the dynamics are determined by a quasicontinuum term, which is due to lattice (intramode) anharmonicity. The most interesting feature of the modified Fano model seems to be its potential ability to describe the recurrence of phonon amplitudes [6], i.e., sudden interruptions in the time evolution produced by the quasicontinuum term [27], as well as the complex nature of the asymmetry parameter q observed in the time domain [9, 28].

3. Conclusions

In summary, we have presented evidence of Fano line shapes for large-amplitude coherent phonons in Bi. They result from interference effects between a discrete phonon state and a broad continuum. A similar type of quantum interference has without doubt gone unnoticed in several ultrafast pump–probe experiments. Our measurements in the time domain over a wide temperature and excitation level range have allowed the determination of phonon self-energy for two optical phonons in bismuth. To explain the data obtained we suggest that the continuum responsible for the interference is formed by both the electronic and lattice degrees of freedom, with their relative importance dependent on the timescale.

Acknowledgments

This work was supported by the Russian Foundation for Basic Research (05-02-19910 and 07-02-00148), the Japan Society for Promotion Science (a collaborative grant together with grants 17540305 and 18340093), as well as by the Iketani Science Technology Foundation.

References

[1] Fano U 1961 *Phys. Rev.* **124** 1866
[2] Hase M, Kitajima M, Constantinescu A M and Petek H 2003 *Nature* **426** 51
[3] DeCamp M F, Reis D A, Bucksbaum P H and Merlin R 2001 *Phys. Rev.* B **64** 092301
[4] Hase M, Kitajima M, Nakashima S and Mizoguchi K 2002 *Phys. Rev. Lett.* **88** 067401
[5] Sokolowski-Tinten K, Blome C, Blums J, Cavalleri A, Dietrich C, Tarasevitch A, Uschmann I, Förster E, Kammler M, Horn-von-Hoegen M and von der Linde D 2003 *Nature* **422** 287
[6] Misochko O V, Hase M, Ishioka K and Kitajima M 2004 *Phys. Rev. Lett.* **92** 197401
[7] Roeser C A D, Kandyla M, Mendioroz A and Mazur E 2004 *Phys. Rev.* B **70** 212302
[8] Murray É D, Fritz D M, Wahlstrand J K, Fahy S and Reis D A 2005 *Phys. Rev.* B **72** 060301(R)
[9] Misochko O V, Ishioka K, Hase M and Kitajima M 2006 *J. Phys.: Condens. Matter* **18** 10571
[10] Misochko O V, Lu R, Hase M and Kitajima M 2007 *Sov. Phys.—JETP* **104** 245
Misochko O V, Lu R, Hase M and Kitajima M 2007 *Zh. Eksp. Teor. Fiz.* **131** 275–85 (in Russian)
[11] Zijlstra E S, Tatarinova L L and Garcia M E 2006 *Phys. Rev.* B **74** 220301(R)
[12] Falkovsky L A and Mishenko E G 1997 *JETP Lett.* **66** 195
[13] Tangney P and Fahy S 2002 *Phys. Rev.* B **65** 054302
[14] Ishioka K, Kitajima M and Misochko O V 2006 *J. Appl. Phys.* **100** 093501
[15] Zeiger H J, Vidal J, Cheng T K, Ippen E P, Dresselhaus G and Dresselhaus M S 1992 *Phys. Rev.* B **45** 768
[16] Merlin R 1997 *Solid State Commun.* **102** 207
[17] Stevens T E, Kuhl J and Merlin R 2002 *Phys. Rev.* B **65** 144304
[18] Abstreiter G, Cardona M and Pinczuk A 1984 *Light Scattering in Solids* vol IV, ed M Cardona and G Guentherodt (Berlin: Springer) p 5
[19] Hunsche S, Wienecke K, Dekorsy T and Kurz H 1995 *Phys. Rev. Lett.* **75** 1815
[20] Hase M, Mizoguchi K, Harima H, Nakashima S and Sakai K 1998 *Phys. Rev.* B **58** 5448
[21] Bansal M L and Roy A P 1986 *Phys. Rev.* B **33** 1526
[22] Abrikosov A A and Falkovski L A 1963 *Sov. Phys.—JETP* **16** 769
[23] Gonze X, Michenaud J P and Vigneron J P 1990 *Phys. Rev.* B **41** 11827
[24] Lie Y and Allen R E 1995 *Phys. Rev.* B **52** 1556
[25] Rzazewski K and Eberly J H 1983 *Phys. Rev.* A **27** 2026
[26] Agarwal G S and Agassi D 1983 *Phys. Rev.* A **22** 2254(R)
[27] Karoly E and Eberly J H 1985 *J. Chem. Phys.* **82** 1841
[28] Misochko O V, Hase M, Ishioka K and Kitajima M 2005 *JETP Lett.* **82** 426